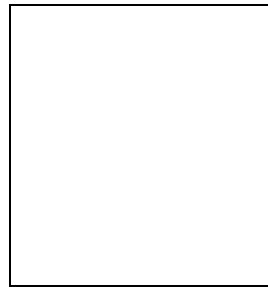


INDIRECT DARK MATTER SEARCH: COSMIC POSITRON FRACTION MEASUREMENT FROM 1 TO 50 GEV WITH AMS-01

H. GAST, J. OLZEM, and ST. SCHAEL

*I. Physikalisches Institut, RWTH Aachen,
Sommerfeldstraße 14, 52074 Aachen, Germany*



A new measurement of the cosmic ray positron fraction $e^+/(e^+ + e^-)$ in the energy range of 1-50 GeV is presented. The measurement is based on data taken by the AMS-01 experiment during its 10 day space shuttle flight in June 1998. A proton background suppression in the order of 10^6 is reached by identifying converted bremsstrahlung photons emitted from electrons and positrons.

1 Introduction

Over the past decades, cosmic ray physics has joined astronomy as a means to gather information about the surrounding universe. Of the few particles that are stable and thus able to cross the vast interstellar distances, electrons and positrons are of particular interest.

Electrons are believed to be accelerated in shock waves following supernova explosions. Their spectrum is subsequently altered by inverse Compton-scattering off cosmic microwave background photons, synchrotron radiation due to the galactic magnetic field, bremsstrahlung processes in the interstellar medium, and finally, modulation in the solar magnetosphere. Thus, they serve as an important probe of cosmic ray propagation models. On the other hand, positrons are secondarily produced in the decay cascades of π^+ , created in hadronic interactions of cosmic ray protons with the interstellar medium, which yields an e^+/e^- ratio of roughly 10 %.

In addition to these classical sources, positrons may also originate from more exotic ones. Among the most important problems in modern cosmology is the nature of dark matter. Based on observations of the cosmic microwave background, supernovae of type IA, and galaxy clustering, among others, the standard model of cosmology now contains a density of non-luminous matter exceeding that of baryonic matter by almost a factor of five¹. The most promising candidate for dark matter is a stable weakly interacting massive particle predicted by certain

supersymmetric extensions to the standard model of particle physics², and called neutralino χ . Positrons and electrons will then be created in equal numbers as stable decay products of particles stemming from χ - χ -annihilations, for instance in the galactic halo. Such a process would constitute a primary source of positrons. Therefore, a measurement of the positron fraction is also motivated by the prospect of indirect dark matter detection, especially if combined with other sources of information, such as antiprotons, diffuse γ -rays or – more challenging – antideuterons.

2 The AMS-01 experiment

As a predecessor to the Alpha Magnetic Spectrometer AMS-02, which is to be operated on the International Space Station (ISS) for at least 3 years, the AMS-01 experiment was flown on the Space Shuttle *Discovery* from June 2nd to 10th, 1998.

The AMS-01 experiment is shown in fig. 1. It consisted of a cylindrical permanent magnet with a bending power of 0.14 Tm^2 and an acceptance of $0.82 \text{ m}^2\text{sr}$. The magnet bore was covered at the upper and lower end each with two orthogonal layers of scintillator paddles, forming the time of flight system (TOF), which provided a fast trigger signal as well as a measurement of velocity and charge number. Mounted inside the magnet volume, the tracking device consisted of six layers of double-sided silicon strip detectors with an accuracy of $10 \mu\text{m}$ in the bending coordinate. The inner magnet surface was lined with the scintillator panels of the anticoincidence system (ACC) serving as a veto counter against particles traversing the magnet wall. For velocity measurements, AMS-01 had a two-layered aerogel threshold Čerenkov counter (ATC) mounted underneath the lower TOF layer, allowing e^+/p discrimination below $3 \text{ GeV}/c$. A low energy particle shield covered the experiment to absorb particles below $5 \text{ MeV}/c$, while a multi layer insulation blanket (MLI) served as a protection against space debris and solar radiation. The radiation thickness of all materials above or below the tracking device, not including the Space Shuttle, sums up to 18.2% or 19.1% of a radiation length, respectively. A detailed description of the experiment is given elsewhere³.

3 Conversion of bremsstrahlung photons

The main challenge of cosmic ray positron measurements is the suppression of the vast proton background. As it is known from previous measurements^{3 4}, the flux of cosmic ray protons exceeds that of positrons by a factor of 10^4 in the momentum range of $1 - 50 \text{ GeV}/c$. Hence, in order to keep the proton contamination of positron samples below 1%, a proton rejection of 10^6 has to be reached. Since the ATC subdetector of AMS-01 provided a sufficient single track proton rejection only for energies below 3 GeV , a different approach has been chosen for this analysis. It relies on the identification of bremsstrahlung emission through photoconversion. Due to the inverse quadratical dependence on the particle mass of the cross section, bremsstrahlung emission is suppressed by a factor of more than $3 \cdot 10^6$ for protons with respect to positrons.

Fig. 1 shows the principle of a converted bremsstrahlung event signature. Here, a primary positron enters the detector volume from above and emits a bremsstrahlung photon in the first TOF scintillator layer. The photon then converts into an electron positron pair, for example, in the second TOF layer. Because of the low fraction of momentum which is typically carried away by the photon, the secondary particles have lower momenta than the primary. Therefore, in the bending plane projection, the secondaries tend to form the left and right tracks, while the primary remains in the middle.

Both bremsstrahlung and photon conversion are closely related electromagnetic processes whose energy angle distributions can be calculated with the Bethe-Heitler formalism. In the relativistic limit, the angle of photon emission as well as the opening angle of pair production

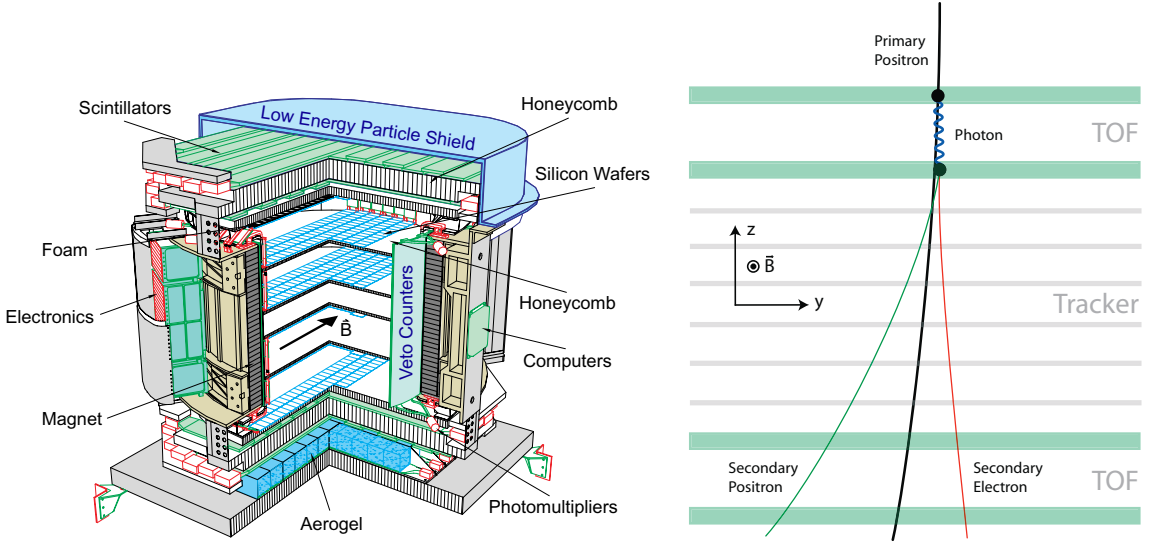


Figure 1: *Left:* The AMS-01 experiment. The tracker layers are equipped asymmetrically. *Right:* Schematic view of a converted bremsstrahlung event caused by a positron going top-down.

show distributions with a most probable value of $\theta_0 \approx 1/\gamma$, γ being the Lorentz factor of the emitting particle or the electron positron pair, respectively. In the GeV energy range, these values fall below the accuracy limit of the track reconstruction induced by multiple scattering, and thus are practically equal to zero.

The dominant background is caused by electrons with wrongly reconstructed momentum sign, as well as by protons undergoing hadronic reactions in the material distribution of the experiment. In the latter case mesons are produced, which mimic the 3-track signature of converted bremsstrahlung events. For example, in the reaction $pN \rightarrow pN\pi^+\pi^- + X$, beneath additional undetected particles X , the charged pions can be misidentified as an electron positron pair. Besides this, neutral pions produced in reactions of the type $pN \rightarrow pN\pi^0 + X$ decay into two photons, one of which may escape undetected. If the remaining photon converts, the conversion pair forms a 3-track event together with the primary proton. However, the invariant mass of the mesons and primary protons is typically at the scale of the pion mass, leading to emission angles significantly larger than zero.

4 Analysis

In order to gain the highest possible selection efficiency, it is mandatory to apply sophisticated track and vertex finding algorithms which are particularly customized for the signature of converted bremsstrahlung^{5 6}.

Analysis and suppression of background mainly rely on the evaluation of the topology and geometrical properties of the reconstructed events, and are therefore based on data from the tracker. Additionally, cuts on data from the TOF system are applied. However, substantial parts of the analysis deal with measures to account for the environmental circumstances under which the AMS-01 experiment was operated, especially the effect of the geomagnetic field.

4.1 Suppression of dominant background

For the suppression of background, the fact is used that bremsstrahlung and photon conversion imply small opening angles of the particles at the vertices. In order to make these angles independent of the frame of reference, the corresponding invariant mass is calculated according

to

$$m_{inv}^2 = 2 \cdot E_1 \cdot E_2 \cdot (1 - \cos \theta), \quad (1)$$

where θ , E_1 and E_2 denote the opening angle and the energies of the primary particle and the photon, or the conversion pair, respectively.

The distributions of the invariant masses are shown in fig.2. For events with negative charge, which represent a largely clean electron sample, they reveal a narrow shape with a peak at zero. This is in perfect agreement with Monte Carlo results. In case of events with positive total charge, consisting of positrons and background, the distributions also show a peak at zero, but additionally a long tail towards higher invariant masses caused by the proton background. In

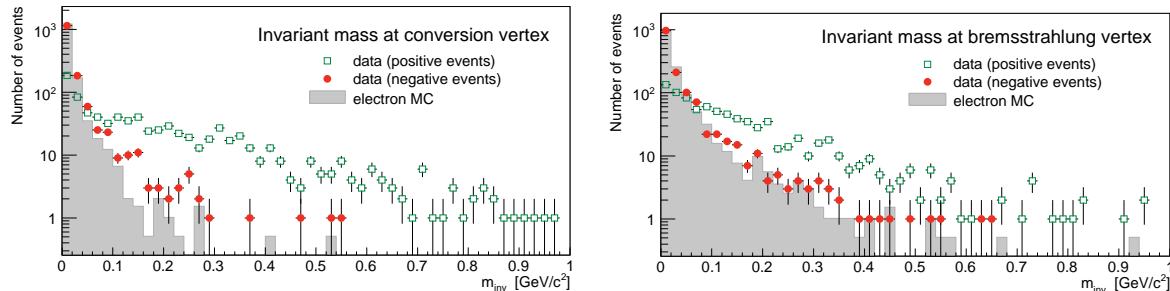


Figure 2: The distribution of the invariant mass at the conversion vertex (*left*) and at the bremsstrahlung vertex (*right*) for data (*dots*) and electron Monte Carlo (*shaded histogram*).

order to discriminate against background events, cuts are applied on the invariant masses. The cuts are parameterized as ellipses in the invariant mass plane.

The efficiency achieved reaches a flat maximum at approximately 20 GeV/c. Towards higher momentum, the decreasing cluster separation approaches the resolution limit of the silicon strip detectors. At low momentum, by contrast, secondary particles may be deflected such that they generate multiple separated hits in the TOF scintillators, which are rejected by the trigger logic of the experiment.

4.2 Geomagnetic cutoff

Energy spectra of cosmic rays are modulated by the geomagnetic field. Depending on the incident direction and the geomagnetic coordinates of the entry point into the magnetosphere, particles with momenta below a certain cutoff are deflected by the magnetic field and cannot reach the Earth's proximity. Hence, below geomagnetic cutoff the particles detected by AMS-01 must originate from within the magnetosphere. They were mostly produced as secondaries through hadronic interactions and trapped inside the Earth's radiation belts.

To discriminate against these secondaries, particle trajectories were individually traced back from their measured incident location, angle and momentum through the geomagnetic field by numerical integration of the equation of motion⁷. A particle was rejected as a secondary if its trajectory once approached the surface of the Earth, and thus originated from an interaction with the atmosphere. Particles which did not reach a distance of 25 Earth radii within a reasonable time were considered as trapped and also rejected.

5 Correction for irreducible background

The distribution of protons in the invariant mass plane does not vanish in the signal region. The same applies to the background from misidentified electrons. Consequently, a small fraction of background events will not be rejected by the cut on the invariant masses. This remaining

irreducible background has to be corrected for. This has been accomplished using Monte Carlo simulations.

The approach used is to run the analysis on an adequate number of proton and electron Monte Carlo events as if they were data, determine the amount and momentum distribution of particles that are misidentified as positrons, and subtract these from the raw positron counts obtained from data. However, such a comparison of Monte Carlo and data requires the adjustment of several properties of the simulated events: neither have they been affected by the geomagnetic field, nor is their input spectrum exactly equal to the true fluxes.

The influence of the geomagnetic field has been introduced to the Monte Carlo particles by folding the distribution of measured momenta with the normalized livetime function (see section 7). Deviations of the incident momentum spectrum $\phi_{MC}(p)$ of Monte Carlo particles from the true fluxes $\phi_D(p)$ measured by AMS-01^{3,8} are corrected for by reweighting the event variables with the ratio $\phi_D(p)/\phi_{MC}(p)$.

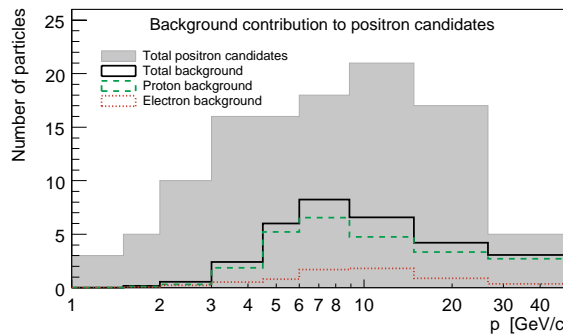


Figure 3: Momentum distribution of the positron candidates including background, and the estimated background contribution from protons and misidentified electrons.

The number of proton Monte Carlo events is scaled to the data by using the sidebands of the invariant mass distributions, while the electron scaling can be determined directly from the candidate sample in the data. Then, the background contribution to the number of positron candidates can be calculated. Fig. 3 shows the total background correction as a function of momentum, separately indicating the contributions from protons and misidentified electrons. They amount to 24.9 and 6.4 events, respectively.

6 Positron fraction

The positron fraction $e^+/(e^+ + e^-)$ is calculated from the electron counts and corrected positron counts for each energy bin. It is shown in fig. 4 in comparison with earlier results and a model calculation based on purely secondary positron production.

Due to the complexity of the positron fraction computation, taking into account 2 sources of background, and low statistics, a Bayesian approach based on Monte Carlo simulation has been chosen for the determination of statistical errors.

In the positron fraction – as a ratio of particle fluxes – most sources of systematic error, such as detector acceptance or trigger efficiency, naturally cancel out. Only sources of error which are asymmetric with respect to the particle charge have therefore to be considered.

The systematic error from background correction can be estimated by evaluating the deviation of the scaled Monte Carlo background from the data in the invariant mass plane. With a binning coarse enough to flatten statistical fluctuations, the mean deviation outside the signal region, i.e. $m_{inv} > 0.25 \text{ GeV}/c^2$ at both vertices, leads to a systematic error estimate of 20 % of the background events. This value is then propagated to the positron fraction for each

momentum bin.

As a consequence of the East West Effect, in combination with the asymmetric layout of the AMS-01 tracker, the product of the detector acceptance and the livetime as functions of the particles' incident direction may vary for positrons and electrons. Even though no deviation of their average livetimes is apparent (see section 7), we account for this effect with a second contribution to the systematic error of the positron fraction. It is estimated from the mean variation of the difference in livetime of positrons and electrons over the detector acceptance. After propagation to the positron fraction, the systematic error due to the East West Effect is well below 10 % for all momentum bins, except for the highest momenta above 26 GeV, where it amounts to approximately 14 % of the positron fraction value.

7 Flux calculation

As a crosscheck to the measurement of the positron fraction, presented above, the absolute incident fluxes of electrons and positrons can be calculated. The electron flux can then be compared to measurements by other experiments and the results obtained previously by AMS-01.

One can calculate the differential flux for a given momentum bin p of width Δp from the measured particle count $N(p, \theta, \phi)$ in this bin, the detector acceptance $A(p, \theta, \phi)$, and the livetime $T(p, \theta, \phi)$. By the term *livetime*, we mean the effective amount of time during which cosmic ray particles coming from outer space have the opportunity to reach the detector. If – as is the case with the AMS-01 downward flux – the livetime is only weakly depending on the direction, the angular distribution of the particle count will follow that of the acceptance. Then, the flux becomes

$$\frac{d\Phi(p)}{dp} = \frac{N(p)}{A(p) \cdot T(p) \cdot \Delta p} \quad (2)$$

While the detector acceptance is determined using a Monte Carlo method based on the GEANT3⁹ simulation of the detector, the live time is calculated from an accurate approach of backtracing virtual particles through the geomagnetic field.

In fig. 4 the fluxes of downward going positrons and electrons, together with results published earlier by AMS-01⁸, and HEAT-e \pm ⁴, are displayed with their statistical errors. The fluxes are in very good agreement with previous measurements over the full momentum range, except for a slight discrepancy in the electron fluxes between 2 and 3 GeV. Here, at low momentum in combination with low statistics, we expect the inaccuracies of the backtracing through the geomagnetic field to become the dominant source of systematic error to the fluxes. However, for the positron fraction as a ratio of particle counts, this effect widely cancels out.

8 Outlook: AMS-02 aboard the International Space Station

The successor to AMS-01, the AMS-02 experiment is currently under construction by the collaboration¹². It will be installed on the International Space Station (ISS) to conduct cosmic-ray spectroscopy with unprecedentedly high precision. The subdetectors that will form part of the experiment are depicted in figure 5 (left).

At its heart, a superconducting magnet of bending power $BL^2 = 0.85$ Tm² forces charged particle onto a curved trajectory, which is measured by the tracker. It consists of eight layers of double-sided silicon microstrip sensors to allow rigidity determination with an accuracy of 20 % at 500 GV. The tracker also has the vital task of finding the charge sign of a particle.

The time-of-flight system, made of two double layers of scintillator panels above and below the tracker, respectively, is used to measure the velocity and charge of a particle and plays a main role in the trigger system. The time resolution obtained is $\Delta t = 100$ ps.

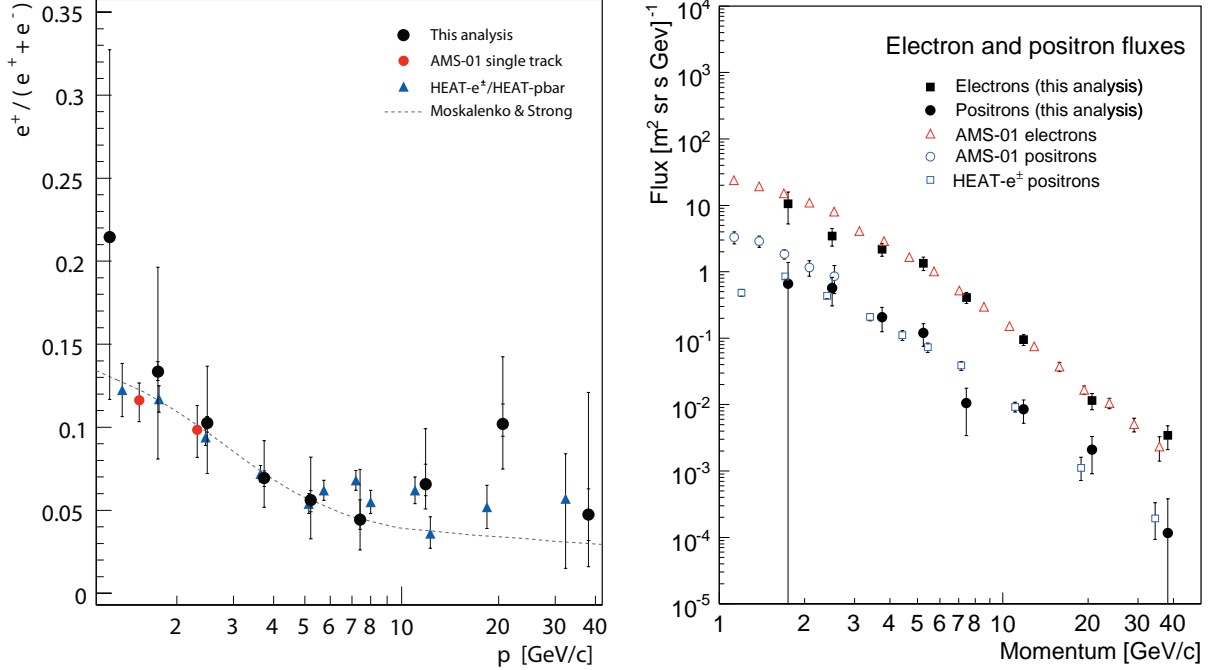


Figure 4: *Left:* The positron fraction $e^+/(e^+ + e^-)$ measured in this analysis, compared with earlier results from AMS-01⁸, HEAT- e^\pm ⁴ and HEAT-pbar¹⁰, together with a model calculation for purely secondary positron production¹¹ (dashed line). The total error is given by the outer error bars, while the inner bars represent the systematic contribution to the total error. *Right:* The fluxes of downward going positrons and electrons measured in this analysis, compared with earlier results from AMS-01⁸ and HEAT- e^\pm ⁴. Error bars denote statistical errors only.

On top of AMS-02, a transition radiation detector (TRD), separates positrons from protons with a rejection power of 10^2 to 10^3 . To achieve this, it uses a radiator fleece and straw drift tubes, filled with a Xe/CO₂ gas mixture, to detect the TR photons.

The proton rejection will be enhanced by a factor of $\mathcal{O}(1000)$ by an electromagnetic sampling calorimeter, made of lead interleaved with scintillating fibres, which is mounted at the bottom of the experiment.

A ring-imaging Čerenkov counter for charge and velocity measurements and an anti-coincidence counter for vetoing lateral tracks complete the detector.

As an example for the capabilities of the AMS-02 detector, the precision that can be obtained for the positron fraction is demonstrated in figure 5 (right) for a one year campaign. In the energy range up to 100 GeV , the statistical error on the data points will be completely negligible. The main scientific goals of AMS-02 can be summarized as follows:

- Indirect search for dark matter in the positron, antiproton and gamma spectra.
- Search for cosmic antimatter ($\overline{\text{He}}$ and heavier nuclei).
- Test propagation models for our Galaxy ($^{10}\text{Be}/^{9}\text{Be}$, B/C, and others).

9 Conclusions

In this paper, we presented a new measurement of the cosmic ray positron fraction up to energies of 50 GeV with the AMS-01 detector. Positrons are identified by conversion of bremsstrahlung photons, an approach which yields an overall proton rejection of more than 10^5 , and allows to extend the energy range accessible to the experiment far beyond its design limits, thus fully

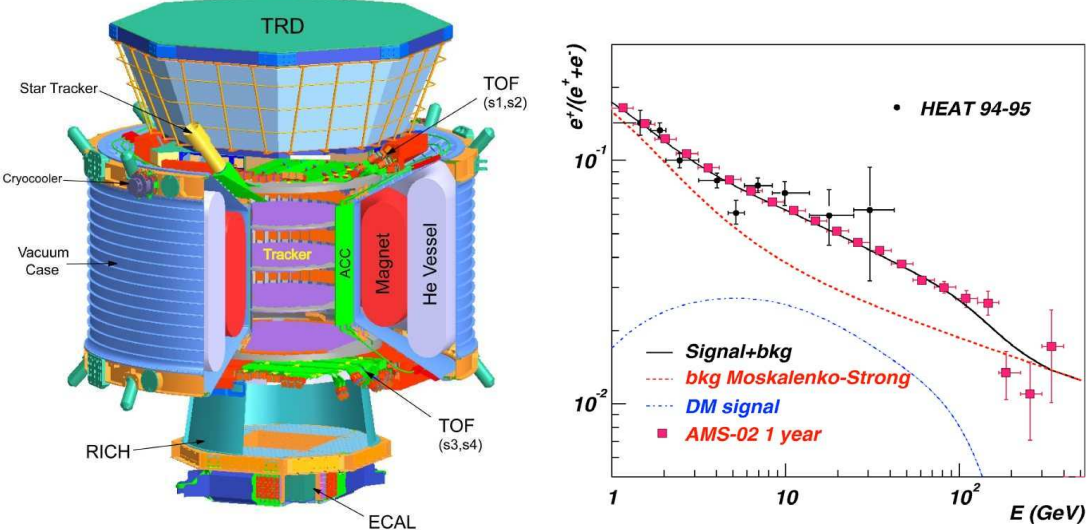


Figure 5: *Left:* View of the AMS-02 subdetectors. *Right:* Statistical uncertainties on positron fraction measurement with one year of AMS-02 data¹³.

exhausting the detector's capabilities. The results are consistent with those obtained in previous experiments at large.

For the reconstruction of converted bremsstrahlung events, customized algorithms for track finding and event reconstruction have to be devised and implemented. We have shown that the background is controllable and the overall uncertainty is dominated by the statistical error due to the low overall cross section of the signal process.

Furthermore, the absolute lepton fluxes have been calculated and found to match the earlier results. This required a new precise and expensive lifetime calculation.

The discovery potential of AMS-02 has been briefly discussed.

Acknowledgements

The authors wish to thank V. Choutko, MIT, and J. Alcaraz, CIEMAT, for their vital help in various aspects of this work. The support of J. Shin and G. Kim, Kyungpook National University, Korea, is gratefully acknowledged.

References

1. S. Eidelmann et al. Phys. Lett. **B 592**, 206 (2004)
2. M. Turner, F. Wilczek. Phys. Rev. **D 42**, 1001 (1990)
3. M. Aguilar et. al. Phys. Rep. **366**, 331 (2002)
4. M. A. DuVernois et al. ApJ **559**, 296 (2001)
5. J. Olzem. PhD thesis in preparation, RWTH Aachen, 2006
6. H. Gast. Diploma thesis, RWTH Aachen, 2004
7. E. Flückiger, E. Kobel. J. Geomag. Geoelectr. **42**, 1123 (1190)
8. J. Alcaraz et al. Phys. Lett. **B 484**, 10 (2000)
9. R. Brun et al. CERN DD/EE/84-1 (1987)
10. J. J. Beatty et al. Phys. Rev. Let. **93**, 241102 (2004)
11. I. V. Moskalenko, A. W. Strong. ApJ **493**, 694 (1998)
12. C. Lechanoine-Leluc. Proc. 29th ICRC Pune (2005) **00**, 101
13. C. Bosio et al. Proc. 12th SUSY Conf. (Tsukuba), 701 (2004)